J|A|C|S
ARTICLES
Published on Web 02/25/2006

Molecular Wires Comprising π-Extended Ethynyl- and Butadiynyl-2,5-Diphenyl-1,3,4-Oxadiazole Derivatives: Synthesis, Redox, Structural, and Optoelectronic Properties

Changsheng Wang,[†] Lars-Olof Pålsson,[‡] Andrei S. Batsanov,[†] and Martin R. Bryce*[,†]

Contribution from the Department of Chemistry and the Department of Physics, University of Durham, Durham DH1 3LE, UK

Received November 23, 2005; E-mail: m.r.bryce@durham.ac.uk

Abstract: 2,5-Diphenyl-1,3,4-oxadiazole (OXD) derivatives with terminal ethynyl- (**4a,b**) and butadiynyl- (**8a,b**) substituents have been synthesized in high yields. 2-Methyl-3,5-hexadiyn-2-ol has not been exploited previously in the synthesis of terminal butadiynes. Crystals of **8a** and **8b** are remarkably stable to long-term storage under ambient conditions. The X-ray crystal structure of **8a** reveals that the butadiyne moieties are spatially isolated by the aromatic moieties, which explains the high stability. Two series of derived π-conjugated molecules, Donor$-$(C$\equiv$C)$_n-$OXD ($n = 1$, 2) and OXD$-$(C$\equiv$C)$_n-$Donor$-$(C$\equiv$C)$_n-$OXD ($n = 1$) [Donor = tetrathiafulvalene (TTF), bithiophene, 9-(4,5-dimethyl-1,3-dithiol-2-ylidene)fluorene, and triphenylamine], have been synthesized using Sonogashira reactions and characterized by X-ray crystallography, cyclic voltammetry, and optical absorption/emission spectroscopy. The electron-withdrawing effect of the OXD units is manifested by a positive shift of the donor oxidation waves in these systems: the butadiynylene spacer ($n = 2$) further shifts the first oxidation waves by 40$-$80 mV compared to analogues $n = 1$. The absorption spectra of TTF$-$OXD hybrids **10d** and **11** are blue-shifted by 80 nm compared to the bithienyl-bridged derivative **10f** and are similar to the butadiynyl$-$OXD building-block **8a**, demonstrating that conjugation is disrupted by a neutral TTF unit. Solutions of the TTF$-$OXD and 9-(4,5-dimethyl-1,3-dithiol-2-ylidene)fluorene$-$OXD hybrids, **10d**, **10g**, **11**, and **13**, are only very weakly fluorescent due to quenching from the electron-donor moieties. In contrast, the triphenylamine$-$OXD hybrids **12a**, **12b**, **14a**, and **14b** are fluorescent; the PLQYs of the butadiynylene derivatives **14a** and **14b** are lower than those of the ethynylene-bridged analogues **12a** and **12b**.

Introduction

In the past two decades, there has been a renaissance in the chemistry of aromatic alkynes, primarily due to the development of the palladium-catalyzed cross-coupling reaction of terminal alkynes with arylhalides (the Sonogashira reaction).[1] This protocol provides an efficient and versatile means of extending $\pi-\pi$ conjugation in organic compounds, affording simplified molecular structures compared with their alkene analogues due to the lack of *Z/E* isomerism around triple bonds. Ethynylene-extended arenes and heteroarenes have been shown to function as nanoscale "molecular wires", with the extent of intramolecular conjugation dependent upon the topology of the π-system and the molecular length.[2] Derivatives of porphyrins,[3] tetrathiafulvalenes (TTFs),[4] and organometallic complexes[5] containing triple bond linkages have been studied recently. Synthetic advances have led to remarkable polyene systems of nanoscale lengths end-capped with organometallic[6] or silyl substituents.[7] However, butadiynylene derivatives, Ar$-$C$\equiv$C$-$C$\equiv$C$-$Ar′, remain fundamentally important targets for studies on opto-electronic properties of carbon-rich backbones,[8] which have not been well-established experimentally.[9]

In this context, we were attracted to 2,5-diaryl-1,3,4-oxadiazole (OXD) derivatives due to their good thermal and chemical stabilities and their high photoluminescence quantum yields.[10] These properties, combined with the electron-deficient nature of the oxadiazole ring, have led to their applications as electron-transporting/hole-blocking materials in organic light-emitting

[†] Department of Chemistry.
[‡] Department of Physics.

(1) (a) Sonogashira, K. In *Comprehensive Organic Synthesis*; Trost B. M., Fleming, I., Eds.; Pergamon Press: Oxford, 1991; vol. 3, p 521. (b) Sonogashira, K. In *Metal-Catalyzed Cross-Coupling Reactions*; Diederich, F., Stang, P. J., Eds.; Wiley-VCH: Weiheim; 1998; p 203. (c) Sonogashira, K. *J. Organomet. Chem*. **2002**, *653*, 46.
(2) (a) Bunz, U. H. F. *Chem. Rev*. **2000**, *100*, 1065. (b) Tour, J. M. *Acc. Chem. Res*. **2000**, *33*, 791. (c) Robertson, N.; McGowan, C. A. *Chem. Soc. Rev*. **2003**, *32*, 96.
(3) (a) Redmore, N. P.; Rubstov, I. V.; Therien, M. J. *J. Am. Chem. Soc.* **2003**, *125*, 8769. (b) Screen, T. O.; Thorne, J. R. G.; Denning, R. G.; Bucknall, D. G.; Anderson, H. L. *J. Mater. Chem*. **2003**, *13*, 2796.
(4) (a) Nielsen, M. B.; Moonen, N. N. P.; Boudon, C.; Gisselbrecht, J.-P.; Seiler, P.; Gross, M.; Diederich, F. *Chem. Commun*. **2001**, 1848. (b) Nielsen, M. B.; Utesch, N. F.; Moonen, N. N. P.; Boudon, C.; Gisselbrecht, J.-P.; Concilio, S.; Piotto, S. P.; Seiler, P.; Günter, P.; Gross, M.; Diederich, F. *Chem.$-$Eur. J*. **2002**, *8*, 3601.
(5) (a) Dembinski, R.; Bartik, T.; Bartik, B.; Jaegerr, M.; Gladysz, J. A. *J. Am. Chem. Soc*. **2000**, *122*, 810. (b) Benniston, A. C.; Harriman, A.; Li, P.; Sams, C. A. *J. Am. Chem. Soc*. **2005**, *127*, 2553.
(6) Mohr, W.; Stahl, J.; Hampel, F.; Gladysz, J. A. *Chem.$-$Eur. J*. **2003**, *9*, 3324.
(7) (a) Eisler, S.; Chahal, N.; McDonald, R.; Tykwinski, R. R. *Chem.$-$Eur. J*. **2003**, *9*, 2542. (b) Eisler, S.; Slepkov, A. D.; Elliott, E.; Luu, T.; McDonald, R.; Hegmann, F. A.; Tykwinski, R. R. *J. Am. Chem. Soc*. **2005**, *127*, 2666.

devices (OLEDs).[11] Low molecular weight OXDs,[12] dendritic,[13] and polymeric derivatives[14] have been studied in this context. Recently, electrochromism has been reported in OXD−TTF hybrids.[15]

The aims of the present work were 2-fold. (1) To develop the synthetic chemistry of OXD derivatives possessing terminal -ethynyl (**4a**,**b**) and -butadiynyl (**8a**,**b**) substituents, with emphasis on the attachment of redox-active chromophores. (2) To probe the extent of π-conjugation through these molecular wires as revealed in their structural, redox, and optoelectronic properties. Our specific targets were a series of linearly conjugated molecules comprising one or two OXD units linked through -ethynyl or -butadiynyl bridges to moieties of different π-electron donating strength, viz., TTF[16] (**10d**, **11**, **13**), thienylene (**10e**), bithienylene (**10f**), 9-[2-(4,5-dimethyl-1,3-dithiolylene)]-2,7-fluorenylene (**10g**), and *N*,*N*-dimethyl-/diphenyl-aminophenyl (**12**, **14**), and for comparison, two electron acceptors, viz. 9-fluorenone (**10a** and **10b**) and 9-dicyanomethylenefluorene (**10c**).

Results and Discussion

Synthesis. The OXD-containing terminal ethynes **4a** and **4b** were synthesized in high yields from the OXD bromides **2** (obtained, in turn, by dehydrative cyclization of **1a** and **1b**) first via Sonogashira couplings with 2-methyl-3-butyn-2-ol[17] (HiPA) followed by deprotection of the precursor compounds **3** in the presence of a catalytic amount of NaOH in toluene[18] (Scheme1). Apart from its low cost, there are two major attractions in using HiPA to synthesize these terminal alkynes. (1) The high polarity of the protected derivatives **3** leads to easy chromatographic separation of the deprotected products **4** from any unreacted **3**. (2) The higher boiling point of HiPA (compared to that of trimethylsilylacetylene) allows higher reaction temperatures, which are required for some unreactive aryl bromides.

The diyne analogue of HiPA, i.e., 2-methyl-3,5-hexadiyn-2-ol,[19] has not been exploited previously in the synthesis of terminal butadiynes. It proved to be an efficient reagent for this purpose, affording **8a**,**b** (Scheme 2) as crystalline solids by analogy with the synthesis of **4a**,**b**. 2-Methyl-3,5-hexadiyn-2-ol was less reactive than HiPA in cross-coupling reactions with aryl bromides **2a**,**b**. Therefore, the iodide derivatives **6a**,**b** were used to avoid high temperatures. It is notable that ***8a**,**b** are stable to routine purification and can be stored under ambient conditions for months without any detectable decomposition*. The unusual high stability of **8a** can be explained by the packing mode in the solid state (as revealed by X-ray analysis: see below).

With **4** and **8** in hand, we proceeded to functionalize the terminal positions with redox-active moieties. The butadiynes **8a**,**b** are particularly attractive building blocks for the synthesis of unsymmetrical 1,4-diarylbutadiyne derivatives, as their cross-coupling reactions preclude any possibility of symmetrical byproducts being formed.[20] Our initial attempt to prepare **10a** by the cross-coupling of **4a** with 2,7-dibromofluorenone under Sonogashira conditions led to self-coupling of **4a** to give **9** (90% yield, Scheme 3). It is well-known that self-coupling of terminal alkynes can occur as a side-reaction alongside cross-coupling,[21] and it is favored when arylbromides are used for the reaction.[22] When the more reactive 2,7-diiofluorenone was used, both **10a**,**b** were isolated in high yields (Scheme 3). Due to the extremely low solubility of 2,7-dibromo-9-(dicyanomethylene)fluorene in organic solvents (requiring boiling DMF), it was not possible to carry out its coupling with **4** or **8**. **10c** was, however, synthesized by a condensation of the fluorenone analogue **10b** with malononitrile.

10d−**g** were similarly obtained in 67−91% yields from the corresponding diiodo compound and reagent **4a** or **b**. Cross-

(8) (a) Karzazi, Y.; Cornil, J.; Brédas, J. L. *Nanotechnology* **2003**, *14*, 165. (b) Tour, J. M.; Cheng, L.; Nackashi, D. P.; Yao, Y.; Flatt, A. K.; St. Angelo, S. K.; Mallouk, T. E.; Franzon, P. D. *J. Am. Chem. Soc.* **2003**, *125*, 13279. (c) Cornil, J.; Karzazi, Y.; Brédas, J. L. *J. Am. Chem. Soc.* **2002**, 124, 3516. (d) Seminario, J. M.; Derosa, P. A.; Bastos, J. L. *J. Am. Chem. Soc.* **2002**, *124*, 10266.

(9) (a) Biswas, M.; Nguyen, P.; Marder, T. B.; Khundkar, L. R. *J. Phys. Chem. A* **1997**, *101*, 1698. (b) Rogers, D. W.; Matsunaga, N.; Zavitsas, A. A.; McLafferty, F. J.; Liebman, J. F. *Org. Lett.* **2003**, *5*, 2373. (c) Rogers, D. W.; Matsunaga, N.; McLafferty, F. J.; Zavitsas, A. A.; Liebman, J. F. *J. Org. Chem.* **2004**, *69*, 7143. (d) Jarowski, P. D.; Wodrich, M. D.; Wannere, C. S.; Schleyer, P. v. R.; Houk, K. N. *J. Am. Chem. Soc.* **2004**, *126*, 15036.

(10) Schulz, B.; Bruma, M.; Brehmer, L. *Adv. Mater.* **1997**, *9*, 601.

(11) Reviews: (a) Kraft, A. *Liebigs Ann./Recueil.* **1997**, 1463. (b) Kraft, A.; Grimsdale, A. C.; Holmes, A. B. *Angew. Chem., Int. Ed.* **1998**, *37*, 402. (c) Mitschke U.; Bäuerle, P. *J. Mater. Chem.* **2000**, *10*, 1471. (d) Hughes, G.; Bryce, M. R. *J. Mater. Chem.* **2005**, *15*, 94.

(12) (a) Adachi, C.; Tokito, S.; Tsutsui, T.; Saito, S. *Jpn. J. Appl. Phys.* **1988**, *27*, L713. (b) Wang, C.; Jung, G.-Y.; Batsanov, A. S.; Bryce, M. R.; Petty, M. C. *J. Mater. Chem.* **2002**, *12*, 173. (c) Chien, Y.-Y.; Wong, K.-T.; Chou, P.-T.; Cheng, Y.-M. *Chem. Commun.* **2002**, 2874.

(13) Cha, S. W.; Choi, S.-H.; Kim, K.; Jin, J.-I. *J. Mater. Chem.* **2003**, *13*, 1900.

(14) (a) Peng, Z.; Bao, Z.; Galvin, M. E. *Chem. Mater.* **1998**, *10*, 2086. (b) Chen, Z.-K.; Meng, H.; Lai, Y.-H.; Huang, W. *Macromolecules* **1999**, *32*, 4351. (c) Wang, C.; Kilitziraki, M.; Palsson, L.-O.; Bryce, M. R.; Monkman, A. P.; Samuel, I. D. W. *Adv. Funct. Mater.* **2001**, *11*, 47. (d) Shu, C.-F.; Dodda, R.; Wu, F.-I.; Liu, M. S.; Jen, A. K.-Y. *Macromolecules* **2003**, *36*, 6698.

(15) Wang, C.; Batsanov, A. S.; Bryce, M. R. *Chem. Commun.* **2004**, 578.

(16) For reviews of TTF chemistry see: (a) Segura, J. L.; Martín, N. *Angew. Chem., Int. Ed.* **2001**, *40*, 1372. (b) Bryce, M. R. *J. Mater. Chem.* **2000**, *10*, 589. (c) Nielsen, M. B.; Lomholt, C.; Becher, J. *Chem. Soc. Rev.* **2000**, *29*, 153.

(17) (a) Havens, S. H.; Hergenrother, P. M. *J. Org. Chem.* **1985**, *50*, 1763. (b) MacBride, J. A. H.; Wade, K. *Synth. Commun.* **1996**, *26*, 2039.

(18) Ames, D. E.; Bull, D.; Takunda, C. *Synthesis* **1981**, 364.

(19) Gusev, I.; Kucherov, V. F. *Bull. Acad. Sci. USSR Div. Chem. Sci. (Engl. Transl.)* **1962**, 995.

(20) Unsymmetrically substituted 1,3-butadiynes have been efficiently synthesized via Pd-catalyzed cross-coupling of 1,3-diynylzincs (Negishi, E.; Hata, M.; Xu, C. *Org. Lett.* **2000**, *2*, 3687) or via alkylidine carbenoid rearrangements (Shi Shun, A. L. K.; Chernick, E. T.; Eisler, S.; Tykwinski, R. R. *J. Org. Chem.* **2003**, *68*, 1339).

(21) Sonogashira, K.; Tohda, Y.; Hagihara, N. *Tetrahedron Lett.* **1975**, *16*, 4467.

(22) Chow, H.-F.; Wan, C.-W.; Low, K.-H.; Yeung, Y.-Y. *J. Org. Chem.* **2001**, *66*, 1910. A self-coupling method has been developed on the basis of Sonogashira conditions without using aromatic halides. (Batsanov, A. S.; Collings, J. C.; Fairlamb, I. J. S.; Holland, J. P.; Howard, J. A. K.; Lin, Z.; Marder, T. B.; Parsons, A. C.; Ward, R. M.; Zhu, J. *J. Org. Chem.* **2005**, *70*, 703.) The presence of adventitious oxygen due to incomplete air exclusion from the reaction vessel is likely to assist the formation of **9**. However, to the best of our knowledge, self-coupling as a major reaction under Sonogashira conditions in the presence of an arylhalide partner is unusual. For **4a**, this could arise due to the increased acidity of the ethynyl hydrogen caused by the electron-withdrawing OXD unit. It is known that less acidic terminal ethynes are less reactive to oxidative self-couplings, and the reaction yields could be improved by the addition of a small amount of strong base (ref 1). In other words, the higher the acidity of a terminal arylacetylene, the higher the yield of self-coupling. Semiempirical calculations (PM3, HyperChem, Version 6.03, Hypercube, Inc., 2000: all calculations terminated at the RMS gradient of 0.01 kcal $Å^{-1}$ mol^{-1}) indicated that **4a** had the smallest net charge (−0.148) on the terminal *sp* carbon atom, compared with those of 4-fluorophenylacetylene (−0.157), TMSA (−0.198), and 4-(phenylethynyl)phenylacetylene (−0.163); i.e., **4a** was the most acidic of these four compounds. We make this comparison because the less acidic TMSA (Lewis, J.; Raithby, P. R.; Wong, W.-Y. *J. Organomet. Chem.* **1998**, *556*, 219), 4-fluorophenylacetylene, and 4-(phenylethynyl)phenylacetylene have been cross-coupled with 2,7-dibromofluorenone under similar conditions. (Ipaktschi, J.; Hosseinzadeh, R.; Schlaf, P.; Eckert, T. *Helv. Chim. Acta* **2000**, *83*, 1224). In addition, the acetylides of **4** and the diacetylides of **8** were less reactive to nucleophilic reactions with ketones and aldehydes than were standard alkyl and aryl acetylenes, which may also be because of the higher acidity of these OXD acetylenes (hence lower nucleophilicity of their derived acetylides). (Kreher, D.; Batsanov, A. S.; Wang, C.; Bryce, M. R. *Org. Biomol. Chem.* **2004**, *2*, 858). Self-coupling of **8a**, in the absence of an aromatic halide, gave the tetrayne analogue of **9** in 40% yield: details will be published separately.

Scheme 1. Synthesis of OXD−ethynes **4**

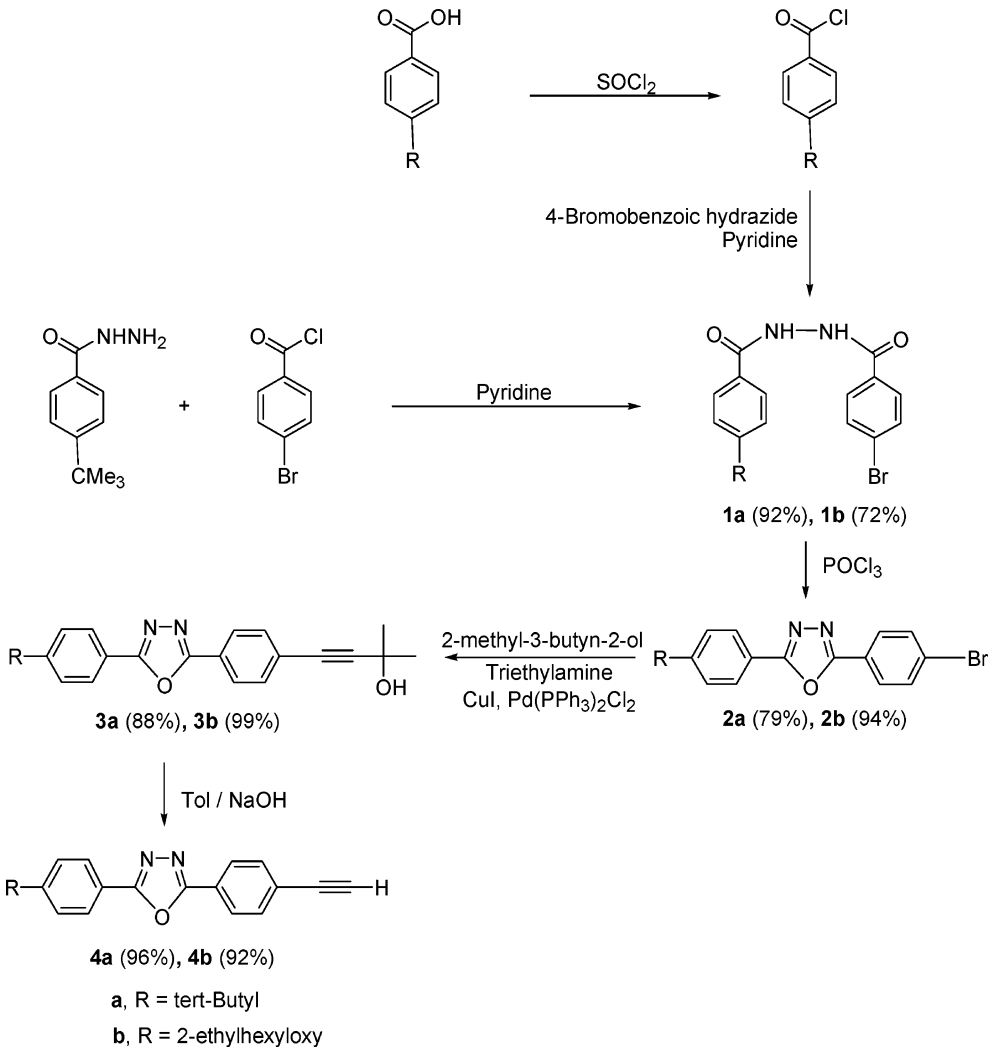

coupled OXD−TTF hybrids **11** and **13** were synthesized (64 and 32% yields, respectively) by the reaction of **4a** and **8b** with iodo−trimethyl−TTF[23] (Schemes3 and 4). In the ^{1}H and ^{13}C NMR spectra of **11** and **13**, the signals from the methyl groups on the TTF moieties were significantly broadened by the presence of a trace amount of acid in commercial $CDCl_3$, leading to cation radical formation by protic doping. However, sharp spectra of **13** were obtained in $CDCl_3$ treated with a grain of solid NaOH. Due to the relatively higher oxidation potential of **10d** compared to those of **11** and **13**, its spectra were less sensitive to the acidity of the solvent, and the signals of the TTF protons were sharp in fresh $CDCl_3$.

The *N*,*N*-dimethyl-/diphenyl-aminophenyl derivatives **12a**,**b** and **14a**,**b** were obtained in moderate yields from reactions of **4** and **8**, respectively, with *N*,*N*-dimethyl- or *N*,*N*-diphenyl-4-iodoaniline.

X-ray Crystallography of 8a, 9, 10g, 11, and 14a. 8a (Figure 1) adopts a nearly planar conformation. The oxadiazole ring is inclined to the benzene rings *i* and *ii* by 5.1 and 3.2°, respectively. All non-hydrogen atoms, except two methyl groups, lie in one plane with an average deviation of 0.06 Å and a maximum of 0.22 Å. The molecules are packed into an infinite stack, parallel to the *x* axis. Each pair of adjacent molecules in the stack is related by an inversion center, the interplanar separations alternating between 3.50 and 3.56 Å. The terminal ethynyl group forms a C−H···N(1) hydrogen bond [C−H 0.94(2), H···N 2.48(2) Å, CHN angle 138(1)°], linking molecules into an infinite chain, parallel to the [1 1 0] direction. **8a** is only the fourth structurally characterized compound with an aryl−C≡C−C≡CH moiety (see below).

9 (Figure 1) has crystallographic C_i symmetry. Unlike the rest, it is substantially nonplanar. Even excluding all methyl groups, the average deviation of non-hydrogen atoms from the mean plane is 0.24 Å with the maximum of up to 0.6 Å. The oxadiazole ring forms dihedral angles of 18.6 and 17.6° with the two adjacent benzene rings *i* and *ii*, respectively. Overall, the molecule adopts an S-shape: the terminal C(benzene)−C(*t*-Bu) bond forms an angle of 126.5° with the central C≡C−C≡C moiety. The total length of the molecule (by van der Waals shape) is ca.35 Å.

10g crystallizes from chloroform as a 1:3 solvate (Figure 1). The molecule of **10g** adopts an approximately planar conformation, except for both 2-ethylhexyl groups, which are intensely disordered. The maximum length of the molecule (in van der Waals shape) is 51 Å, whereas the length of its planar part [between the centers of the O(3) and O(4) atoms] is 36.6 Å. In

(23) John, D. E.; Moore, A. J.; Bryce, M. R.; Batsanov, A. S.; Howard, J. A. K. *Synthesis* **1998**, 826.

Scheme 2. Synthesis of OXD−butadiynes **8**

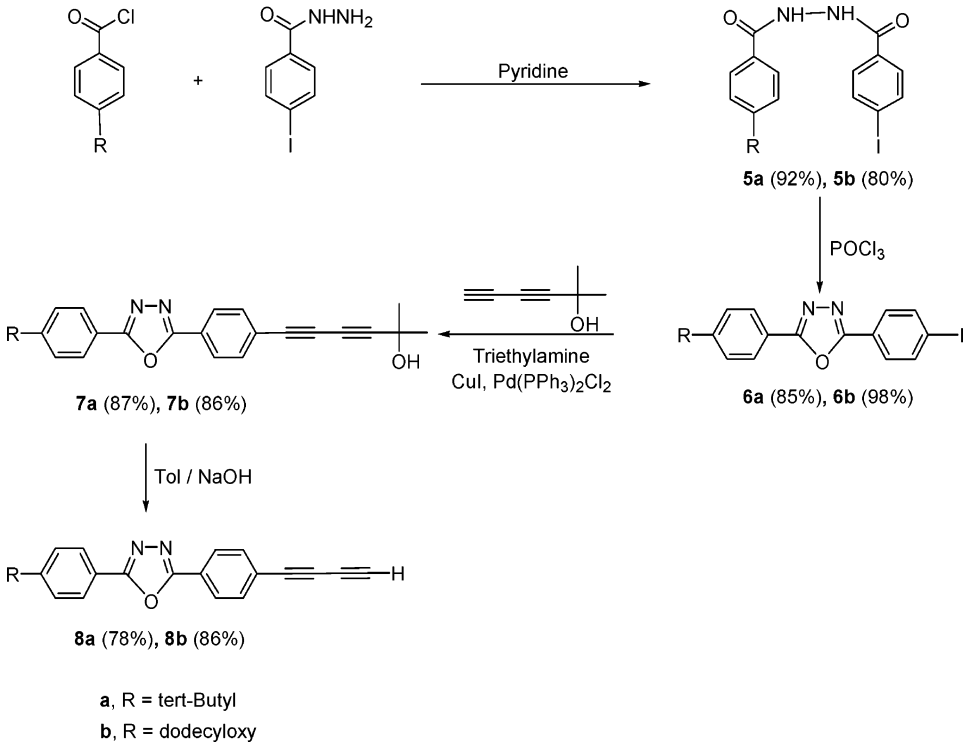

the latter part, the average deviation of atoms from the mean plane is 0.16 Å, and the maximum deviation is 0.38 Å. The 1,3-dithiole ring is folded by 3.4° along the S···S vector; its S(1)CS(2) moiety is inclined by 5.5° to the fluorene system, which is planar within experimental error. The inter-ring dihedral angles are: *i*/*ii* 5.4, *ii*/*iii* 1.6, *iii*/*iv* 9.3, *v*/*vi* 12.5, *vi*/*vii* 7.2, and *vii*/*viii* 10.3°. The structure being triclinic, all molecules are parallel; they are stacked in brickwork-type layers parallel to the (1 0 0) plane, with interplanar separations alternating between 3.26 and 3.39 Å. Three independent chloroform molecules (one of them rotationally disordered) are linked to the **10g** molecule via hydrogen bonds with the N(2), N(4), and S(2) atoms.

In **11** (Figure 1), all non-hydrogen atoms, except two methyl groups, are coplanar with the average deviation of 0.08 Å and the maximum one of 0.24 Å. The TTF moiety shows a chairlike distortion, folding along the S(1)···S(2) and S(3)···S(4) vectors by 5.9 and 3.5°, respectively. The angles between the oxadiazole ring and the benzene rings *i* and *ii* are 10.8 and 1.2°; that between ring *ii* and the C_2S_2 moiety *iii* is 8.6°. The molecules pack in a herringbone fashion, with the planes of adjacent molecules forming a dihedral angle of 16.3°.

14a (Figure 1) has the total van der Waals length of ca. 30 Å. The oxadiazole ring is inclined to the benzene rings *i* and *ii* by 6.6 and 4.0°, respectively. The angle between rings *ii* and *iii* is 13.9°. The N(3) atom has a planar-trigonal geometry, its plane inclined by 51.4° to that of ring *iii*, due to steric repulsion from the phenyl groups *iv* and *v*. With the exception of the latter and of two methyl groups, all non-hydrogen atoms lie in one plane with a mean deviation of 0.09 Å and a maximum of 0.26 Å. The molecules are stacked into centrosymmetric, head-to-tail dimers in which the oxadiazole ring of one molecule overlaps with the benzene ring *ii* of another and vice versa, with a mean interplanar separation of 3.35 Å.

The structure of **8a** is particularly interesting and merits further discussion. Very few terminal (in contrast with disubstituted) butadiyne derivatives are known, obviously due to their lower chemical stability. A survey of the May 2005 version of the CSD[24] revealed only six such compounds, three with aryl−C≡C−C≡CH[25] and three with C(sp^3)−C≡C−C≡CH[26] moieties, and a number of transition metal complexes where the bonding along the M−C≡C−C≡CH chain may differ substantially from the diyne pattern, due to back donation from the metal atom. Disubstituted butadiynes are important precursors of polydiacetylenes, and the conditions for their topochemical (crystal lattice-controlled) polymerization have been extensively studied.[27] The polymerization requires close proximity between the butadiyne moieties, with a continuous chain of intermolecular C1···C4′ contacts or of alternating C1···C1′ and C4···C4′ contacts. This can be ideally achieved by a slanted arrangement of parallel butadiyne moieties, so that a vector connecting their centers is ca. 4.9 Å long ("repeat distance", *d*) and forms an angle (Φ) of 45° with the butadiyne rod. Such packing is adopted by 1-resorcinol-1,3-butadiyne in the crystals of its monohydrate (d = 5.09 Å, Φ = 45°, C1···C4′ distance 3.64 Å) and its 1:1 molecular complex with an oxalamide (d = 4.72 Å, Φ = 54°, C1···C4′ distance 3.95 Å), both of which undergo topochemical polymerization with a transformation of a single crystal into a single crystal, as proven by X-ray

(24) Allen, F. H.; Taylor, R. *Chem. Soc. Rev.* **2004**, *33*, 463.
(25) (a) Inoue, K.; Koga, N.; Iwamua, H. *J. Am. Chem. Soc.* **1991**, *113*, 9803. (b) Inoue, K.; Iwamua, H. *Adv. Mater*. **1992**, *4*, 801. (c) Classen, J.; Gleiter, R.; Rominger, F. *Eur. J. Inorg. Chem.* **2002**, 2040.
(26) (a) Keller, M. B.; Rzepa, H. S.; White, A. J. P.; Williams, D. J. *First Electron. Conf. Trends in Org. Chem*. 1995; p 50 (cit. from CSD, refcode NAMLAO). (b) Murty, K. V. S. N.; Vasella, A. *Helv. Chim. Acta* **2001**, *84*, 939. (c) Xi, O.; Fowler, F. W.; Lauher, J. W. *J. Am. Chem. Soc.* **2003**, *125*, 12400.
(27) (a) Baughmann, R. H. *J. Appl. Phys.* **1972**, *43*, 4362. (b) Enkelmann, V. *Chem. Mater*. **1994**, *6*, 1337. (c) Coates, G. W.; Dunn, A. R.; Henling, L. M.; Dougherty, D. A.; Grubbs, R. H. *Angew. Chem., Int. Ed*. **1997**, *36*, 248.

Scheme 3. Cross-Coupling Reactions of OXD−ethynes **4**

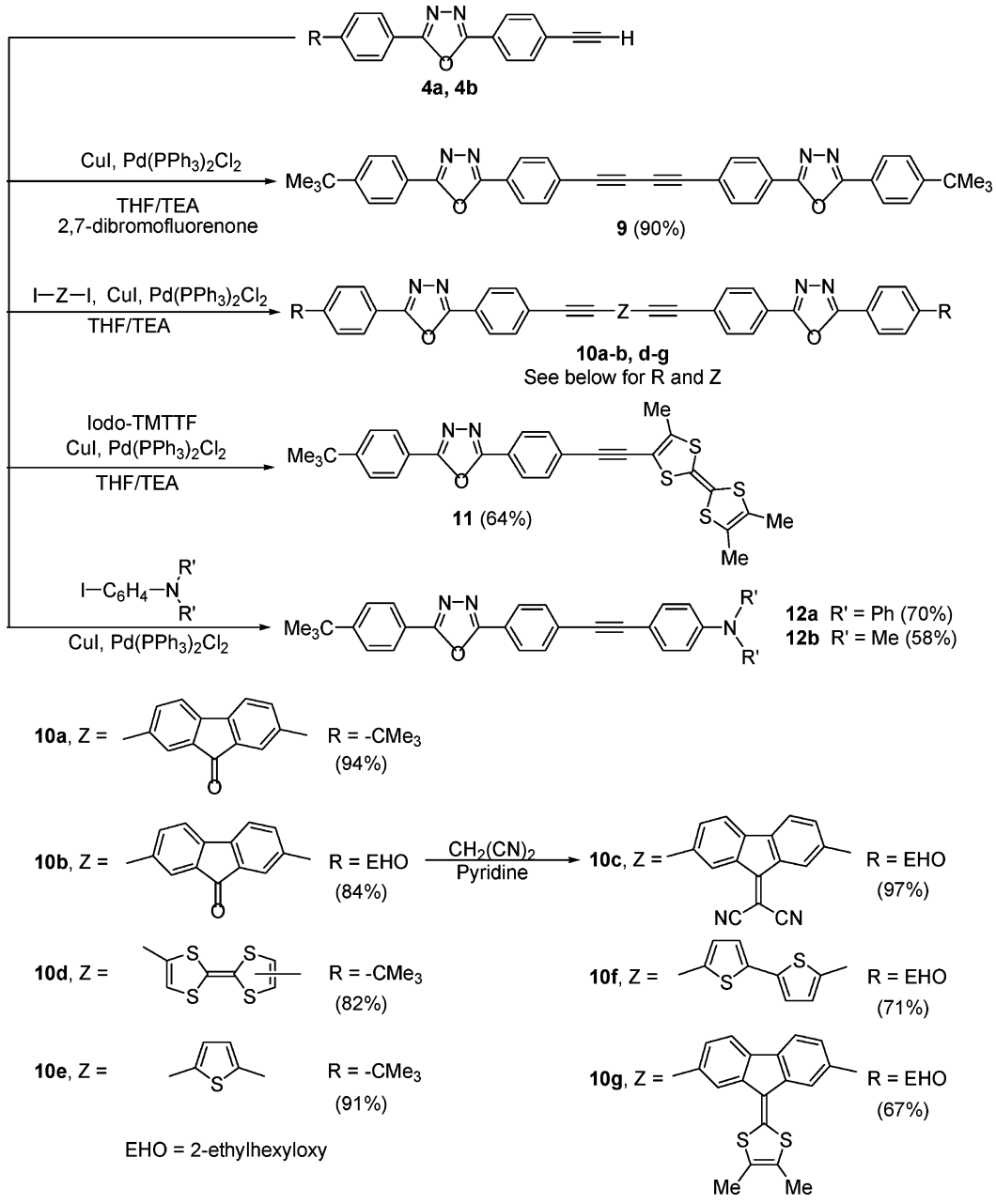

diffraction studies of both the starting and the polymerized samples.[27c] An alternative prearrangement for polymerization is a close packing of parallel molecules without any slanting (d = 3.4 Å, Φ = 90°), which has seldom been achieved for disubstituted butadiynes (actually, with d = 3.7 Å, Φ = 75−82°)[26c] and, to our knowledge, never for terminal butadiynes.The topochemical polymerization has been reported for 3-[Bu^{t}N(OH)]-4-ClC_6H_3C≡C−C≡CH, but the evidence is less conclusive.[26a] The polymer has not been structurally characterized, and we found it difficult to reconcile the description of the monomer structure in this paper with the atomic coordinates deposited in the CSD (refcode VOVLIB). The authors reported that polymerization propagated along the *a/c* diagonal of the crystal and associated it with a chain of butadiyne moieties along this direction, with alternating contacts C1···C4′ of 4.55 Å and C4···C4′ of 4.72 Å. We have calculated the C1···C4′ contact of 4.49 Å and found no C4···C4′ distance shorter than 5.99 Å. There is, in fact, a C1···C1′ contact of 4.72 Å in the proposed diagonal direction, but the mutual orientation of the molecules is quite awkward. In any case, neither a C1···C4′, C4···C4′ nor C1···C4′, C1···C1′ succession provides a chemically meaningful path for polymerization, and the contact distances involved are much longer than what is usually regarded as the upper limit for topochemical polymerization (ca. 4 Å).[27c]

In the structure of **8a**, the butadiyne moieties form no continuous chains, only discrete antiparallel pairs (molecules are symmetrically related via an inversion center) with d = 5.39 Å and Φ = 75.7°. The intermolecular distances therein, C1···C4′ 5.39 Å and C1···C1′ 5.76 Å, are even longer than in the aforementioned structure. From all other sides, the butadiyne moiety is screened by benzene rings, a methyl group, and a heterocycle of three adjacent molecules. Thus, the structure offers no conditions for solid-state polymerization. To confirm this postulation, the crystals of **8a** were heated at 10 °C/min to

Scheme 4. Cross-Coupling Reactions of OXD−butadiynes **8**

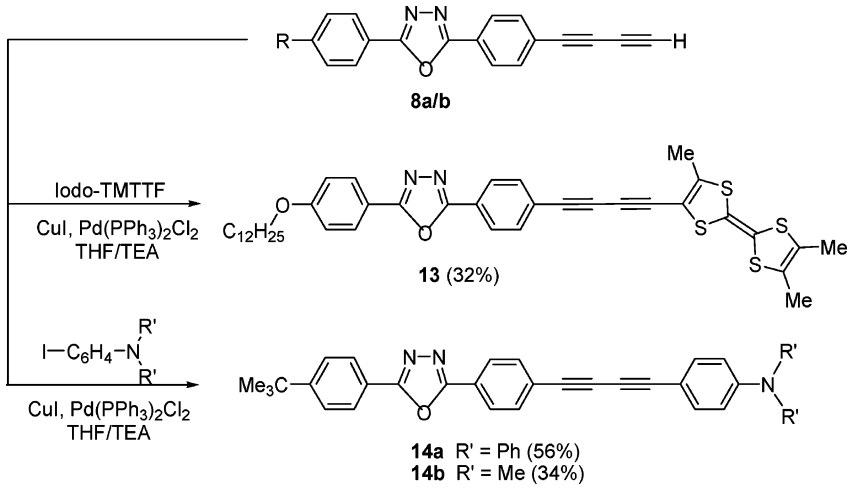

145 °C, and the high temperature was held for an additional 0.5 h. No obvious thermally induced reaction was observed under an optical microscope. Subsequent heating to >160 °C led to a darkening of the solid, and the resultant black solid did not melt until 320 °C.

UV−Vis Absorption Spectra. The solution UV−vis absorption spectra of **4** and **8** and their coupled products **9**−**14** were recorded, and representatives are shown in Figure 3a−d.

Figure 3a shows the spectra of the bisOXD−butadiyne **9** and the bisOXD−TTF derivative **10d** compared with their building blocks **4a** and **8a**, respectively. Despite the longer molecular length of **10d** compared to that of **9**, the λ_{max} of **10d** (326 nm) was 24 nm shorter than that of **9** (350 nm) and similar to that of **8a** (324 nm). These data demonstrate that there is conjugation of the two OXD moieties through the butadiyne bridge in **9**, whereas neutral TTF disrupts the conjugation, and in molecule **10d**, there is essentially no conjugation between the two OXD moieties. It could also be considered that these two OXD moieties in **10d** communicate in a way similar to cross-conjugating functional groups in oligo(enynes).[28] The conjugation length of **10d** was equivalent to that of **4a**, extended by only one of the TTF peripheral double bonds. This conclusion also explains the essentially superimposable spectra of **10d** and **11** (λ_{max} = 326 and 328 nm, respectively, the latter is shown in Figure 3d). The 2-nm red-shift for **11** could be due to the substituent effects of the methyl group on the same side of the TTF moiety. A comparison with the spectra of **10e**,**f** is also informative. The additional thiophene ring in the bisOXD−ethynyl bithiophene **10f** led to a 27-nm red-shift of λ_{max} compared with the thiophene analogue **10e** (Figure 3d), indicating extended conjugation through the longer bridge. However, although the TTF-bridged molecule **10d** (λ_{max}= 326 nm) is geometrically longer than **10e** and comparable with **10f**, its primary λ_{max} was 53 nm shorter than that of **10e** (379 nm) and 80 nm shorter than that of **10f** (406 nm). This arises again because the neutral TTF bridge distorts the conjugation between the OXD−acetylene segments.

Figure 3b shows that the primary absorption bands of the three fluorenone analogues **10a**,**c**,**g** have similar features. This is because the substitution of the O-atom at the 9-position of the fluorenone unit does not affect the conjugation lengths of the backbones. The shoulder on the low-energy side of **10g** is characteristic of TTF/1,3-dithiole-containing compounds and could be attributed to exciplex formation.

The aniline derivatives **12a**,**b**, and **14a**,**b** all exhibited two-band absorption features with comparable oscillation strength, although **14** showed clear fine structures (Figure 3c). Varying the amino substituents from phenyl to methyl in **12a**,**b** led to 5- and 9-nm blue-shifts for each band, respectively, which were consistent with the UV spectra in cyclohexane of triphenylamine (λ_{max} = 301 nm)[29] and dimethylaniline (λ_{max} = 295 nm).[30] However, the phenyl-to-methyl substitution in **14** resulted in very small shifts in the opposite direction (ca. 3 nm for both bands), indicating a difference in donor−acceptor interactions through the butadiyne bridge.[31] The existence of the additional low-energy absorption bands in **12** and **14** can be explained by the fact that these molecules comprise conjugatively linked acceptor (A)−donor (D) units (OXD and amino, respectively). Such an A−D combination significantly reduces HOMO−LUMO gaps,[32] a feature which is also seen in the solution electrochemical behavior of these compounds (see below, Figure 7d). Broad, low-energy absorptions occur at ca. 450 nm for **10a**, **10b**, **10d**, **11**, and **13**. For **10a**,**b**, this band (ϵ ca. 7000) is attributed to $n-\pi^*$ transitions associated with the carbonyl group; for **10d**, **11**, and **13** (ϵ 800−2000), they are assigned to sulfur-related $n-\pi^*$ transitions, which are typical of many substituted 1,3-dithiole and TTF derivatives.

Emission Spectra. Both **12a** and **14a** showed single-wave emission bands at 466 and 479 nm, respectively, in chloroform solutions at 310 K, whether the excitations were placed at the high-energy or the low-energy absorption regions. The photoluminescence excitation (PLE) spectra of **12a** and **14a** were compared to the 1-transmission (1-T) spectra. The ambient temperature PLE and (1-T) spectra of **12a** (Figure 4, upper) are very similar, confirming an energy transfer process across the C≡C bond system of at least 97% efficiency. In contrast, the PLE and (1-T) spectra of **14a**, under the same conditions,

(28) Tykwinski, R. R.; Zhao, Y. M. *Synlett* **2002**, 1939.

(29) Schiemenz, G. P.; Nielsen, P. *Phosphorus Sulfur* **1984**, *21*, 259.
(30) Mangini, P. *J. Chem. Soc.* **1956**, 4954.
(31) Graham, E. M.; Miskowski, V. M.; Perry, J. W.; Coulter, D. R.; Stiegman, A. E.; Schaefer, W. P.; Marsh, R. E. *J. Am. Chem. Soc.* **1989**, *111*, 8771.
(32) (a) Williams, D. H.; Fleming, I. *Spectroscopic Methods in Organic Chemistry*, 4th ed.; McGraw-Hill Book Company: London, 1989; p 20. (b) Roncali, J. *Chem. Rev.* **1997**, *97*, 173. (c) Perepichka, D. F.; Bryce, M. R. *Angew. Chem., Int. Ed.* **2005**, *44*, 5370.

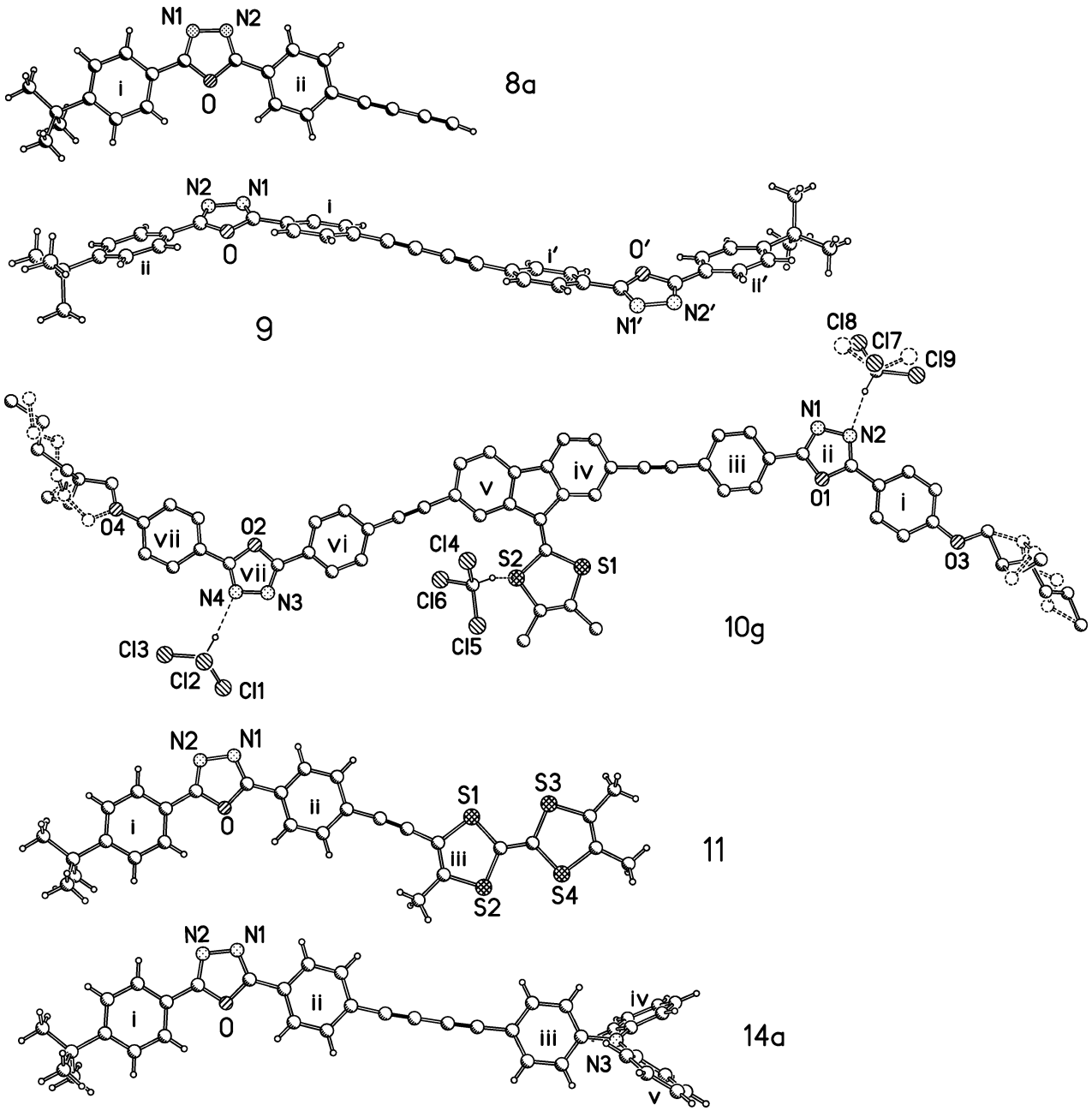

Figure 1. Molecular structures of **8a**, **9** (primed atoms are generated by the inversion center), **10g**·3$CHCl_3$, showing the disorder (H atoms are omitted for clarity, except those which form hydrogen bonds), **11**, and **14a**.

were different in the 400-nm region. Normalizing the PLE and (1-T) at ~375 nm gives an 88% transfer efficiency upon excitation in the ~330 nm band (Figure 4, lower). These data, therefore, suggest a difference in energy transfer efficiency between **12a** and **14a** at ambient temperatures.

A comparison of the spectra obtained at 77 K shows that the transfer efficiency in **14a** was only 72% of the corresponding efficiency in **12a**, for excitation in the 320-nm region. The same experiments carried out for the methyl analogues **12b** and **14b** gave similar results (data not shown) that confirm that the effects observed can be attributed to the butadiynylene bridge rather than to substituents on the aniline moieties.

We have also observed that the wavelengths and intensities for the emission bands for both **12** and **14** were significantly temperature dependent. In the case of **12a** (Figure 5), the PL λ_{max} had a small red-shift at T > 150 K followed by a sharp blue-shift starting at ca. 125 K, as the temperature decreased. The PL intensity decreased gradually with the red-shift then sharply increased, accompanying the blue-shift. The PL intensity of **12a** at 77 K was about 2.5-fold of magnitude higher than at 150 K. The same trend for the temperature dependence was also observed for **14a**, and the PL intensity increased even more significantly: at 77 K it was more than 10 times stronger than at ca. 225 K. It is also noteworthy that the blue-shift for **14a** started at a temperature 80 K higher than that for **12a** (ca. 150 K for **12a** and 230 K for **14a**, Figure 5b). Varying the substitution at the aniline moieties (viz. from **12a** to **12b** and **14a** to **14b**) did not alter the trends of temperature dependence. This again confirms that the observed effects originated from the ethynylene/butadiynylene bridge rather then the functional group.

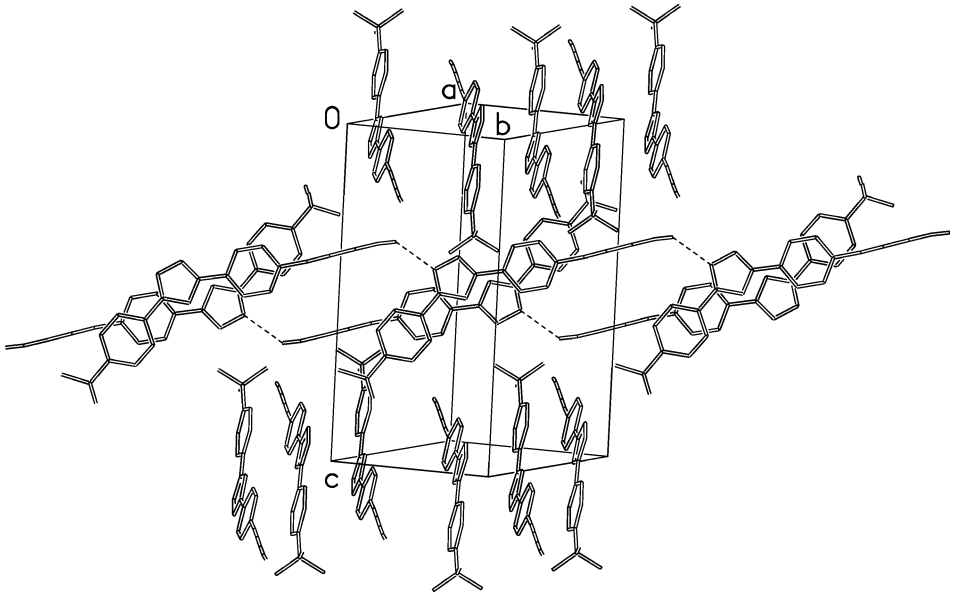

Figure 2. Crystal packing of **8a**, showing −C≡C−H···N hydrogen bonds (other H atoms are omitted for clarity).

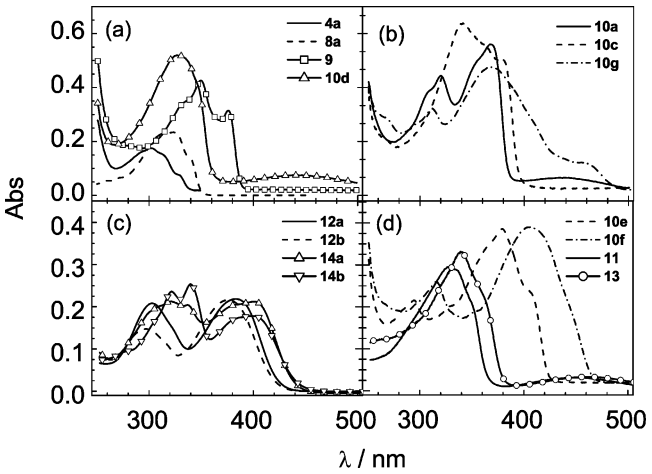

Figure 3. UV−vis absorption spectra of **4a**, **8a**, **9**, **10a**, **10c**−**g**, **11**, **12**, **13**, and **14** in DCM solution (1×10^{-5} mol·dm^{-3}).

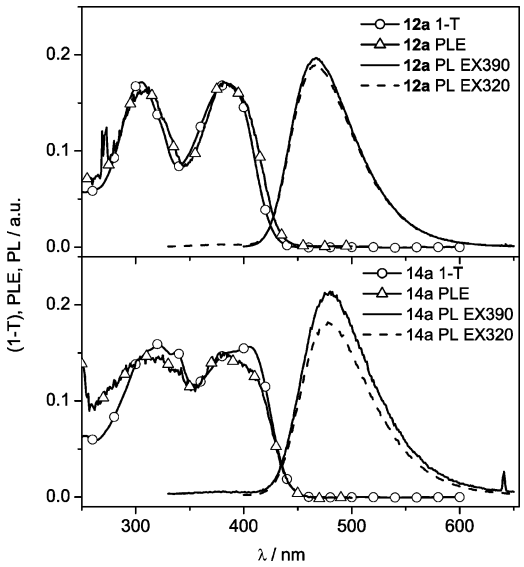

Figure 4. Photoluminescence excitation (PLE), emission (PL), and 1-transmission (1-T) spectra of **12a** and **14a** in chloroform solution at ambient temperature.

A possible explanation for the T-induced blue-shift could be that excitation-/decay-associated structural reorganization of the atoms became difficult in the solvent matrix, and hence, the transition/decay modes changed upon freezing. Semiempirical level (PM3) calculations for **12a** and **14a** could explain this situation. Figure 6 shows their frontier orbitals. For both compounds, the HOMOs reside mostly on the aniline side, whereas the LUMOs reside mostly on the OXD fragment. The HOMO-to-LUMO transition or the LUMO-to-HOMO decay demand significant structural reorganization in the molecules, which will become harder, or even impossible, as the solvent matrix is formed at low temperature. Accordingly, a transition/decay, which requires a smaller degree of structural reorganization (e.g., those between the LUMO and the HOMO-1, Figure 6), will take place. A blue-shift is, therefore, expected in this case. As the degree of structural reorganization of **14** is larger than that of **12**, this blue-shift process starts at higher temperature for **14** than for **12**.

The photoluminescence quantum yields (PLQYs, relative to an anthracene/ethanol standard) of **12** and **14** probed a further difference between the two structures. For **12a**,**b** the PLQYs were 93 and 89%, whereas for **14a**,**b** the values were 36% and 4%, respectively (λ_{exc} 320 nm). We conclude, therefore, that there is a less efficient transfer of excitation energy from the OXD unit across the butadiynylene bridge than across the ethynylene bridge, independent of the aniline substituents. We assume that the energy in **14**,**b** is lost through a nonradiative de-excitation pathway involving the OXD moiety.

Cyclic Voltammetry. The solution redox properties of **4a**, **8a**, **10b**−**g**, and **11**−**14** have been studied by cyclic voltammetry (CV) (Figure 7 and Table 1). **10d**, **11**, and **13** exhibited reversible TTF-type, two-step, one-electron redox couples between 0 and 1 V (vs Ag/Ag$^+$−acetonitrile) (Figure 7a). Compared with trimethyl−TTF,[33] the half-wave potentials of **11** (0.12 and 0.63 V) and **13** (0.16 and 0.64 V) were anodically shifted by ca. 100 mV, due to the electron-withdrawing OXD−ethynyl or −butadiynyl substituents. The additional ethynylene spacer in **13** resulted in only a small increase in the oxidation

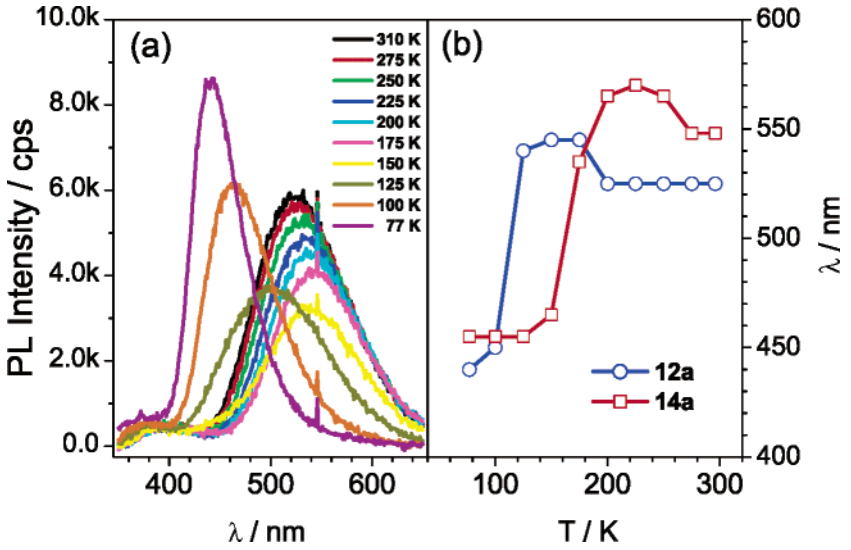

Figure 5. Temperature dependence of the photoluminescence of **12a** and **14a**. (a) PL profiles of **12a** in chloroform−propylene carbonate matrix at different temperatures (λ_{exc} 310 nm). (b) T-λ_{em} dependence of **12a** (λ_{exc} 330 nm) and **14a** (λ_{exc} 340 nm).

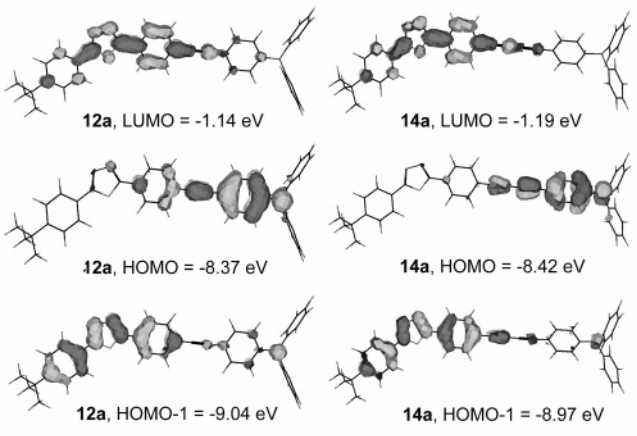

Figure 6. Semiempirical calculated (PM3) frontier orbitals (HOMO and LUMO) and the orbitals immediately below the HOMOs (HOMO-1) of **12a** and **14a**.

potentials (40 mV for the first and 10 mV for the second waves). The oxidation potentials of **10d** were further anodically shifted: the two redox waves appeared at $E^1_{1/2} = 0.31$ V and $E^2_{1/2} = 0.74$ V, due to the additional ethynyl−OXD group combined with the absence of the electron-donating methyls.

In contrast to the TTF systems, **10g** showed only one reversible oxidation wave at $E_{1/2}$ 0.58 V within the same potential range, which is ascribed to the formation of the **10g**$^{\bullet+}$ species. The thienyl and bithienyl derivatives **10e**,**f** exhibited irreversible waves at 1.27 and 0.98 V, respectively (Figure 7b). The irreversibility of these two derivatives was in agreement with the data for 3,4-ethylenedioxythiophene (EDOT) and biEDOT,[34] and the oxidation potentials were in agreement with those of 2,5-diphenylthiophene and 5,5′-diphenylbithiophene[35] in addition to the anodic shift caused by the ethynyl−OXD substitution. Repeated scans of solutions of **10e**,**f** led to significant deposition of the oxidized species rather than polymerization.

The reductive-scan CVs of **10b**,**c** in THF solution are shown in Figure 7c. The first reversible redox wave of **10b** at −1.40 V arises from the fluorenone ketone reduction, whereas the second wave at −1.95 V is associated with the central fluorene units. Due to the strongly electron-withdrawing dicyanomethylene group, both waves of **10c** were anodically shifted by ca. 50 mV ($E^1_{1/2} = -0.83$ V and $E^2_{1/2} = -1.48$ V) when the cathodic scan was limited to −2.0 V, which can be attributed to the formation of **10c**$^{\bullet-}$ and **10c**$^{2-}$ species.[36]

To understand the electrochemical behavior of the cross-coupled derivatives, the CVs of **4** and **8** have to be explained first. Both **4a** and **8a** showed irreversible anodic waves at 1.8 V associated with oxidation of the ethynyl groups, and **4a** showed two poorly resolved reduction waves at ca. −2.3 and −2.45 V, whereas the reduction of **8a** was anodically shifted giving three waves at −2.43, −2.21, and −2.03 V (Figure 7c). These reduction waves are associated with both the triple bonds and the OXD rings. The introduction of aniline groups into **4a** (to afford **12a**,**b**) introduced new irreversible oxidation waves, respectively, at 0.73 V (**12a**) and 0.46 V (**12b**) (Figure 7d, upper). Similar behavior was observed for **14a**,**b** (Figure 7d, lower). The DMF solutions of **12b** and **14b** (both were insoluble in acetonitrile) did not allow the observation of the acetylenic oxidations.

It is noteworthy that, unlike their building blocks (**4** and **8**) and other analogues in this series that are strongly fluorescent, solutions of all the 1,3-dithiole-containing derivatives, namely, **10d**, **10g**, **11**, and **13**, were only very weakly fluorescent, which is in accord with previous observations that TTF is an efficient quencher of fluorescence.[37] We considered that compounds with an oxidation potential more cathodic than that of **10g** (0.66 V vs Ag/Ag$^+$−acetonitrile; Figure 7 and Table 1) could be nonphotoluminescent. However, this is not the case. **12b** and **14b** are oxidized at 0.46 V (**12b**) and 0.54 V (**14b**) respectively, but their solutions, similar to **12a** and **14a**, were fluorescent

(33) Moore, A. J.; Bryce, M. R.; Batsanov, A. S.; Cole, J. C.; Howard, J. A. K. *Synthesis* **1995**, 274.
(34) Sotzing, G. A.; Reynolds, J. R.; Steel, P. J. *Adv. Mater.* **1997**, *9*, 795.
(35) Apperloo, J. J.; Groenendaal, L.; Verheyen, H.; Jayakannan, M.; Janssen, R. A. J.; Dkhissi, A.; Beljonne, D.; Lazzaroni, R.; Bredas, J.-L. *Chem.−Eur. J.* **2002**, *8*, 2384.
(36) (a) Perepichka, I. F.; Kuz'mina, L. G.; Perepichka, D. F.; Bryce, M. R.; Goldenberg, L. M.; Popov, A. F.; Howard, J. A. K. *J. Org. Chem.* **1998**, *63*, 6484. (b) Perepichka, I. F.; Popov, A. F.; Orekhova, T. V.; Bryce, M. R.; Andrievskii, A. M.; Batsanov, A. S.; Howard, J. A. K.; Sokolov, N. I. *J. Org. Chem.* **2000**, *65*, 3053.

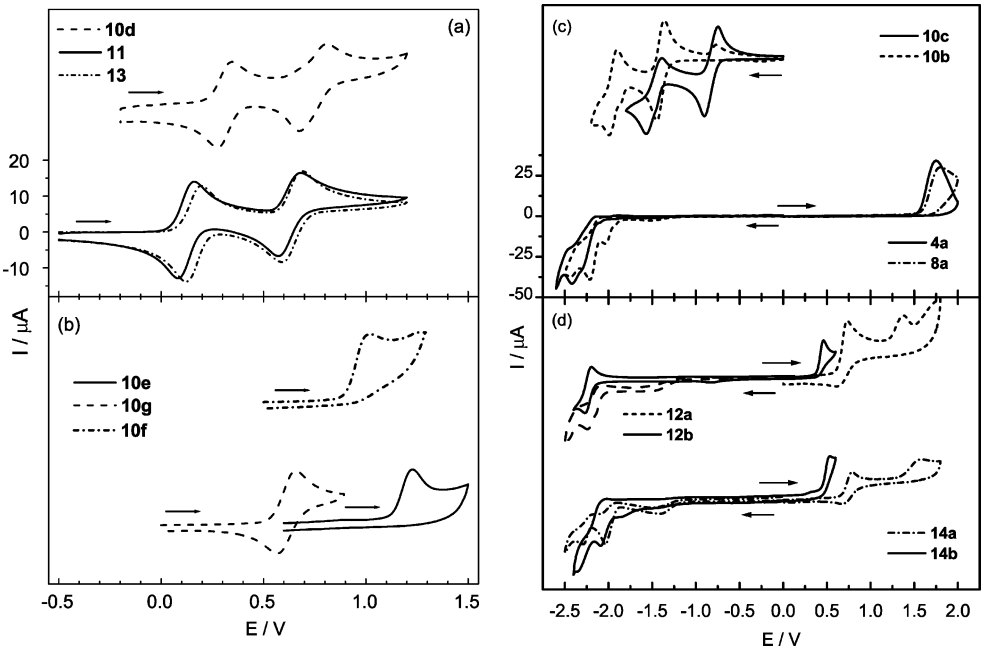

Figure 7. Cyclic voltammograms of: (a) **10d**, **11**, and **13** in DCM; (b) **10f**, **10g**, **10e** in DCM; (c, upper) **10c** and **10b** in THF, (c, lower) **4a** and **8a** in acetonitrile; and (d) **12a** and **14a** in acetonitrile, **12b** and **14b** in DMF. All of the solutions contained 0.1 M $TBAPF_6$ as the supporting electrolyte, and the voltammograms were recorded at 100 mV/sec, using Pt disk ($\Phi = 1.8$ mm) as the working electrode, Pt wire as the counter electrode and $Ag/AgNO_3$−acetonitrile as the reference electrode. Under these conditions in DCM, $E^{1/2}$ of ferrocene was 0.175 V. Due to the irreversibility of **4**, **8**, **12**, and **14** to both reduction and oxidation, the cathodic and anodic scans were performed separately starting from 0 V; the initial scan directions are indicated with arrows.

Table 1. Redox Peak Potentials (vs Ag/Ag^+) of Compounds in Different Solvents

compound	E_{red}^3	E_{red}^2	E_{red}^1	E_{ox}^1	E_{ox}^2
4a[a]		−2.42			1.75
8a[a]	−2.43	−2.21	−2.03		1.80
10b[b]		−1.99	−1.45		
10c[b]		−1.57	−0.90		
10d[c]				0.35	0.81
10e[c]				1.23	
10f[c]				1.02	
10 g[c]				0.66	
11[c]				0.16	0.68
12a[a]		−2.24		0.73	1.38
12b[d]		−2.27		0.46	
13[c]				0.20	0.69
14a[a]	−2.29	−2.03		0.79	1.57
14b[d]	−2.35	−2.10		0.54	

[a] Acetonitrile. [b] THF. [c] DCM. [d] DMF.

(**12** has higher PLQYs than **14**). A most likely explanation for the fluorescence of **12** and **14** is that the LUMO-to-HOMO decay process associated with the *N*,*N*-diphenylaniline units is radiative, whereas the TTF/1,3-dithiole-related relaxations in **10d**, **10g**, **11**, and **13** are nonradiative.[38] *Intra*molecular energy transfer could proceed from the OXD moieties of the excited states to the TTF/1,3-dithiole neutral/radical cation moieties to form nonradiative excited states of **10d**, **10g**, **11**, and **13**. This postulation can be explained by taking **10d** as an example. Neutral **10d** had a weak low-energy absorption maximum at 442 nm in the visible region, whereas the cation radical of **10d** had two absorption bands centered at ca. 435 and 722 nm

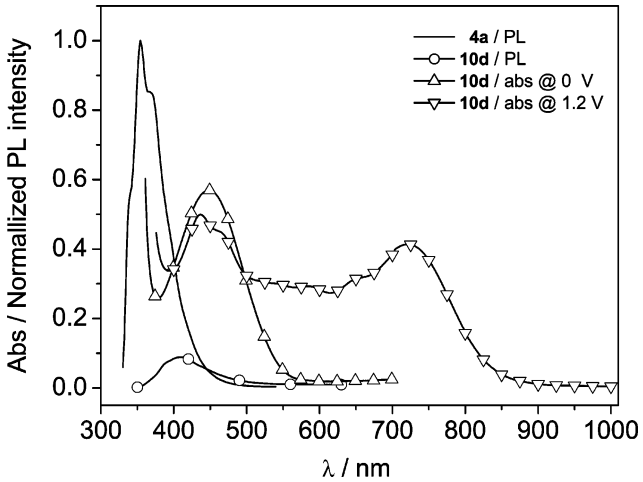

Figure 8. Photoluminescence spectra of **4a** (solid line, λ_{ex} 250 nm), **10d** (circled line, λ_{ex} 300 nm) in chloroform solution, and UV−vis absorption spectra of **10d** in dichloromethane containing 0.1 M $Bu_4N{\cdot}PF_6$ at 0 and 1.2 V applied voltages (vs Pt).

(Figure 8) in a DCM-$TBAPF_6$ electrolyte solution.[13] The low-energy absorption band corresponds to the HOMO−LUMO transition. Whether a charge-transfer process, as proposed,[37] is involved or not, HOMO−LUMO transitions of both neutral and cation-radical **10d** are of lower energy than the emission of the OXD−alkyne building block (**4a**, $\lambda_{em} = 354$ nm), and the energy of the latter emission will be self-absorbed.

Conclusions

We have successfully developed the chemistry of -ethynyl (**4a,b**) and -butandiynyl (**8a,b**) OXD derivatives. Functionalization has been readily achieved at their terminal positions using Pd(II)-catalyzed cross-coupling reactions with a range of redox-active moieties [e.g., TTF, bithiophene, 9-(4,5-dimethyl-1,3-

(37) (a) Wang, C.; Bryce, M. R.; Batsanov, A. S.; Stanley, C. F.; Beeby, A.; Howard, J. A. K. *J. Chem. Soc., Perkin Trans. 2* **1997**, 1671. (b) Farren, C.; Christensen, C. A.; FitzGerald, S.; Bryce, M. R.; Beeby, A. *J. Org. Chem.* **2002**, *67*, 9130. (c) Loosli, C.; Jia, C.; Liu, S.-X.; Haas, M.; Dias, M.; Levillain, E.; Neels, A.; Labat, G.; Hauser, A.; Decurtins, S. *J. Org. Chem.* **2005**, *70*, 4988.

(38) Zimmer, K.; Gödicke, B.; Hoppmeier, M.; Meyer, H.; Schweig, A. *Chem. Phys.* **1999**, *248*, 263.

dithiol-2-ylidene)fluorene, and triphenylamine, etc.] to provide two series of compounds, Donor−$(C\equiv C)_n$−OXD (n = 1, 2) and OXD−$(C\equiv C)_n$−Donor−$(C\equiv C)_n$−OXD (n = 1). The structural, optical, and redox properties of these compounds have provided a unique opportunity to probe conjugation through rigid-rod aryleneethynylene and arylenebutadiynylene wire structures. The following conclusions emerge from this study.

1) Terminal butadiynes are versatile building blocks for unsymmetrical 1,4-diarylbutadiyne derivatives, and the remarkable stability of the terminal butadiynyl-2,5-diphenyl-1,3,4-oxadiazole derivatives **8a**,**b** has been explained by the crystal packing of **8a**.

2) The additional ethynylene group in the butadiynylene derivatives leads to a relatively small, but clearly observable, increase in conjugation length compared to ethynylene analogues.

3) There is less-efficient intramolecular energy transfer through the butadiynylene bridge than the ethynylene bridge in oxadiazole−π−triphenylamine conjugates.

4) π-Conjugation is disrupted by a neutral TTF unit.

Acknowledgment. C.S.W. was funded by EPSRC. L.O.P. acknowledges financial support from CENAMPS. We thank Professor J. A. K. Howard for the use of X-ray facilities and EPSRC for funding the improvement to the X-ray instrumentation.

Supporting Information Available: General experimental methods, synthetic details and characterization data for **1**−**14** and *N*,*N*-diphenyl-4-iodoaniline. X-ray crystallographic file for **8a**, **9**, **10g**, **11**, and **14a** in CIF format. This material is available free of charge via the Internet at http://pubs.acs.org.

JA0577600